

ORIGINAL PAPER

R. W. S. Schneider · J. Lanzen · P. A. Moore

Boundary-layer effect on chemical signal movement near the antennae of the sphinx moth, *Manduca sexta*: temporal filters for olfaction

Accepted: 1 September 1997

Abstract For olfaction to occur, signal molecules must move through the environment from the source to the receptor cells. As molecules approach receptor structures they pass through a boundary layer surrounding those receptor structures. Within boundary layers the interaction between the forces causing chemical dispersion changes. To investigate how the boundary layer changes the dynamics of the chemical signals, we measured chemical dynamics within the boundary layer around the moth antennae using microelectrodes. The results showed that the boundary layer amplified three aspects of the chemical signal: peak height, peak onset, and decay time. Spectral analysis of turbulent signals showed that the temporal aspects of the chemical signal were altered. The boundary layers around the male and female antennae have different effects on the spectrum of chemical temporal fluctuations. Specifically, at a flow speed of 0.12 m s^{-1} , the analysis showed distinct amplification patterns for each sex. Thus, the fluid flow around the antennae functions as a filter, altering the structure of the chemical signal that is arriving at the receptors. The results illustrated in this study show that male and female moths have different physical filters that can alter the information that can be extracted from odor plumes.

Key words Chemoreception · Filters · Fluid flow · *Manduca sexta* · Olfaction

Abbreviations: *Pe* Peclet · *Re* Reynolds

Introduction

An important, yet understudied, step in olfaction is the movement of chemical signals from the environment to

the local vicinity around receptor neurons (Atema 1985, 1988). This movement involves two physical processes: the transport of the chemical signal by fluid flow (Vogel 1983; Cheer and Koehl 1987; Koehl 1993, 1995, 1996) and molecular diffusion (DeSimone 1981; Futrelle 1984). The relative roles that these two physical processes play in the dispersion of a chemical signal are described by the Peclet (*Pe*) number. The *Pe* number is the ratio of dispersion owing to fluid flow to molecular diffusion, and indicates the importance of these characteristics in structuring the three-dimensional distribution of chemical signals. *Pe* numbers greater than one indicate that fluid flow plays the dominant role in dispersion. Conversely, *Pe* numbers less than one indicate that molecular diffusion is the dominant dispersion process. In flow-dominated dispersion, the signals are carried in plumes from a point source upcurrent (Murlis and Jones 1981; Murlis et al. 1991; Moore et al. 1994). In diffusion-dominated dispersion, the random walks of molecules determine the spatial and temporal distribution of chemical signals (Berg 1993). Since most macroscopic organisms and chemosensory appendages operate at *Pe* numbers greater than one, chemical signals are typically dispersed by fluid flow.

For *Pe* numbers larger than one (i.e., flow-dominated dispersion), the Reynolds (*Re*) number describes the pattern of fluid flow. The *Re* number is the ratio of inertial forces to viscous forces and indicates different patterns of flow in systems, such as turbulent or laminar flow. At a high *Re* number, inertial forces dominate and turbulence is generated, while at a low *Re* number (< 1), the viscous forces dominate and turbulence is quickly dampened. The dispersion of chemical signals by turbulence occurs at a much faster rate than dispersion by laminar flow.

The morphology of receptor structures (e.g., antennae) plays a critical role in modifying the flow patterns in the microenvironment immediately surrounding the receptor cells by creating a boundary layer. As fluid flows over a solid surface, the fluid in direct contact with the surface does not flow. This is called the no-slip

R.W.S. Schneider · J. Lanzen · P.A. Moore (✉)
Laboratory For Sensory Ecology,
Department of Biological Sciences,
Bowling Green State University,
Bowling Green, OH 43403, USA
Fax: +1-419 372-2024, e-mail: pmoore@bgnet.bgsu.edu

condition and results in a region of flow called the boundary layer (Vogel 1994). Within the boundary layer, there exists a velocity gradient between the surface (which is zero) and freestream (the maximum velocity). At lower Re numbers, the boundary layers are thicker, but as the Re number increases the boundary layer becomes thinner. The Re number at which an organism maintains its chemosensory appendages dictates the amount of flow that passes through its antenna versus around it (Vogel 1983; Cheer and Koehl 1987; Koehl 1993).

Within the boundary layer, the fluid velocity steadily decreases towards the solid surface. As the fluid velocity decreases, both the Pe and local Re numbers change. As a consequence, the relative contribution of fluid flow and molecular diffusion to chemical transport processes also changes. At the outermost edge of the boundary layer, the Pe number is larger and flow plays a greater dispersal role. Near the surface, the Pe number is smaller, so molecular diffusion becomes more important. Therefore, there is a change from flow to diffusion as the dominant physical process for chemical signal transport near the antenna and within a boundary layer. Since the spatial and temporal distribution of the chemical signals is determined by the interaction between fluid flow and molecular diffusion, the boundary layer can have profound effects on the chemical signal. By altering the dynamics of chemical signal dispersion, the boundary layer will act as a physical filter, changing the dynamics of chemical signals arriving at the receptor cells.

For macroscopic organisms, chemical signals are dispersed and transported by turbulence within the environment. This results in a chemical signal that is patchy in space and time. Over the past decade, the quantification of the spatial and temporal dynamics of chemical signals in turbulent odor plumes has been performed by a number of researchers (Murlis and Jones 1981; Atema 1985; Moore and Atema 1988, 1991; Zimmer-Faust et al. 1988; Murlis et al. 1991; Moore et al. 1994). While these studies have been instrumental in providing insight into the nature of chemical signals, the measurements reflect only a partial understanding of the dynamics of signals as they are perceived by organisms. Boundary layers surrounding receptor appendages and sampling behaviors by organisms will greatly alter the dynamic nature of the signals measured in these studies (Moore et al. 1991).

To examine the filtering effect that boundary layers and fluid flow have on chemical signal structure arriving at receptor cells, we measured chemical dynamics in the boundary layer around the antennae of the moth, *Manduca sexta*, with microelectrodes. We examined the filtering effects of the boundary layer using both pulsatile odors and turbulent odor-plume distributions and examined differences between male and female moths. The goal of this study is to quantify the functional role that boundary layers play in filtering potential information contained within environmental odor signals.

Materials and methods

Modeling air flow in a water medium

To use current electrochemical technology to measure chemical signals (IVEC-10), we used water instead of air as our medium of flow. Since air and water are both fluids, either can be used to model fluid flow if the flow dynamics are the same for each medium (Vogel 1983, 1994). If the Re number of an antenna in air is identical to the Re number of an antenna in water, then the flow patterns of both situations are identical and water can be used to model air flow (Vogel 1994).

The behavior of a fluid in a system is described by the Re number ($Re = ul/v$), where u is velocity, l is length scale, and v is kinematic viscosity of the fluid. For our studies with *M. sexta*, we have taken the diameter of the antennae (0.001 m) as the characteristic length scale. The kinematic viscosity of air is $1.5 \times 10^{-5} \text{ m}^2 \text{ s}^{-1}$ at 20 °C. The Re number for a male antenna in air is 34 at 0.51 m s^{-1} , 100 at 1.5 m s^{-1} , and 226 at 3.4 m s^{-1} . These flow speeds were selected as a range of typical flying speeds for this moth.

Vogel (1983) used a scaling factor to model air flow in water to keep both the flow patterns and forces experienced by a moth antennae in air identical to those experienced in water. We need to reduce velocities by a factor of 28 and increase temperature to 52 °C. Thus, the air speeds of 0.51 , 1.5 , and 3.4 m s^{-1} in air, correspond to 0.018 m s^{-1} , 0.053 m s^{-1} , and 0.12 m s^{-1} in water.

The Pe number indicates the relative contribution of fluid flow and molecular diffusion in chemical dispersion ($Pe = ul/D_m$), where u is velocity, l is length scale, and D_m is the diffusion coefficient. For our studies with *M. sexta*, we have taken the diameter of the antennae (0.001 m) as the characteristic length scale. We used the diffusion coefficient (D_m) of bombykol ($2.5 \times 10^{-6} \text{ m}^2 \text{ s}^{-1}$; Adam and Delbrück 1968). The Pe number for a male antenna in air is 204 at 0.51 m s^{-1} , 600 at 1.5 m s^{-1} , and 1360 at 3.4 m s^{-1} . To approximate the Pe number of a moth antennae in air with one in water, the water was heated to increase the diffusion coefficient. The diffusion coefficient of the molecule changes with temperature according to the relationship $D_m = T * f$ (Adamson 1973). The diffusion coefficient of our tracer molecule, dopamine, is $2 \times 10^{-9} \text{ m}^2 \text{ s}^{-1}$ at 293 K. By increasing the temperature 32 K to 325 K, the diffusion coefficient increased to $2.2 \times 10^{-9} \text{ m}^2 \text{ s}^{-1}$. The Pe numbers under these conditions are 8181, 24090, 54545 at 0.018 m s^{-1} , 0.053 m s^{-1} , and 0.12 m s^{-1} , respectively. While the Pe numbers in water are an order of magnitude greater (≈ 40 -fold), both situations indicate a flow-dominated dispersion.

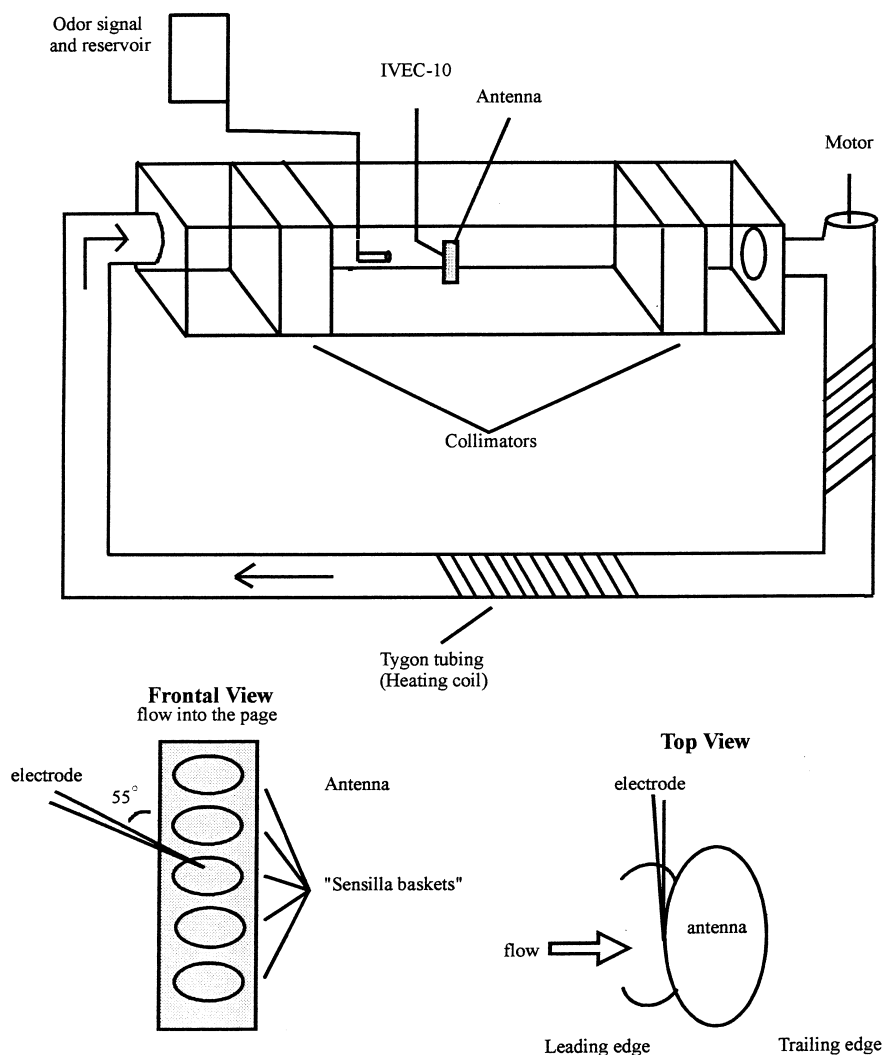
Animals

The *M. sexta* eggs were provided by Dr. Noelle Granger (U.N.C. Chapel Hill), and were reared in the lab on an artificial wheat-germ diet (Bell and Joachimn 1976) in an environmental chamber on a 16L:8D cycle at 26 °C (Keogh and Smith 1991). The heads of adults with the antenna intact were excised and preserved in 95% ethanol 2–3 days after emergence. The animals had a head circumference of $0.68 \pm 0.013 \text{ cm}$ (mean \pm SEM). Male and female antennae were identified using light microscopy. Fine-scale differences in antennal morphology were examined using scanning electron microscopy.

Flow tank

The experiment was conducted in a recirculating flow tank (13 cm \times 14 cm \times 90 cm) constructed with four-inch PVC pipe (Fig. 1). The working section was 4 cm \times 4 cm centered in the flow tank, 20 cm downstream from the entrance collimator and 25 cm upstream from the exit collimator. The working section was located 10 cm downstream from the continuous source and 8 cm downstream from the pulse-signal delivery systems. Under these condi-

Fig. 1 Flume layout with the arrangement of the electrode on the antenna in detail. Front and side view showing placement of the electrode relative to flow and moth antenna



tions, the Re number for the flow tank, dye visualizations, and chemical measures indicate that odor dispersion from a continuous source was turbulent. Water was obtained from a hot-water tap adjusted to 52 °C as measured with a thermometer. The flow tank was drained and refilled after each trial. To maintain the flow tank at 52 °C, Tygon tubing (1/2 inch i.d.) was wrapped around the return pipe and hot water circulated through it. The temperature of the water did not fluctuate more than 2 °C above or below 52 °C for the duration of the experimental trials. The odor signal was stored in a water bath at 52 °C to insure the water in the flow tank and odor signal were at the same temperature. Flow speeds were controlled with an electric motor (model # U-116 Security Universal) with a four-blade prop (blades 45° normal to the shaft), and a variable transformer (model # 3PN1010 Staco Energy) was used to control the motor.

Flow speeds were determined by recording 20 particle velocities in the working section of the flume. The particles were small and neutrally buoyant. Particle velocities were determined by videotaping the working section at different flow speeds and measuring the time it took the particles to travel a designated 5-cm section. The particle speed was correlated with the voltage settings on the transformer to match voltages with flow speeds.

A single right antenna was held in place with a 28-gauge syringe, which pierced the base of the antennae (approximately 0.75 mm depth). The antennae were inserted normal to the flow with the sensillum facing the flow. The syringe and antennae were mounted onto a micromanipulator (Stoelting MM 33) to move the

antennae to the fixed recording electrode in the working section. To minimize additional boundary-layer effects due to the presence of the electrode against the antenna, the electrode was placed at a 90° angle relative to the flow (see Fig. 1). In addition, the electrode tip was placed on the surface of the antenna at an angle of 55° relative to the antennal shaft. The boundary-layer thickness around the electrode by itself and the moth antenna by itself can be found using standard equations for equilibrium boundary-layer thickness around cylinders that are normal to flow (Schlichting 1987). These calculations show that the boundary-layer thickness around the electrode is 3% of the boundary-layer thickness around the moth antenna. From these calculations, it was determined that the electrode had a minimal effect increasing the overall thickness of the boundary layer for the moth antenna.

Recording techniques

Since the introduction of microelectrochemical techniques to aquatic applications, it has become possible to quantify chemical distributions at very small spatial scales and with high temporal resolution (Moore and Atema 1991; Moore et al. 1989, 1991, 1992, 1994). The IVEC-10 recording technique is now a standard practice for these applications and has been used in studies similar to the present study to measure chemical dynamics within other sensory appendages (Moore et al. 1989, 1991). This technique has several advantages for chemosensory applications. These include small

electrode sizes (diameters of 30 μm), fast temporal sampling (up to 200 Hz), and the ability to place electrodes within sensory structures without compromising electrode operation. This technique was originally developed to record neurotransmitter concentrations within the CNS tissue (Gerhardt et al. 1984, 1987).

In this study, electrodes consisted of a 30- μm carbon fiber. The sampling area of the electrode is determined by the exposed carbon epoxy surface area (Adams 1969). Recordings were made at a sampling rate of 10 Hz using the IVEC-10 (In Vivo Electrochemistry Computer System; Medical Systems, Greenvale, NY). Each 100-ms epoch for the 10-Hz sampling rate is composed of a 50-ms epoch at +0.55 V (oxidation) followed by a 50 ms epoch at 0.0 V (reduction). The recording electrodes were sampled every 50 ms: analog-to-digital conversions of the samples occurred at 4 kHz, and data were averaged for the 50-ms time epoch. Further details of recording and digitizing are explained elsewhere (Moore et al. 1989).

Electrodes were calibrated in solutions of dopamine and exhibited excellent linearity over a concentration range of 0.5–100 $\mu\text{mol}\cdot\text{l}^{-1}$ (correlation coefficient; $r^2 > 0.96$). The electrodes actually measure chemical flux in that they are detecting the number of molecular encounters with the electrode's surface per unit time. For the sake of simplicity, we use the term "concentration" to describe the calibrated signal from the electrodes. A more accurate description in flowing systems may be "molecular encounters per unit time". In this way, the electrodes and chemoreceptor cells in a flowing environment detect chemical signals in an identical manner.

Chemical signals for the continuous odor plumes were measured at the base, (5th–7th segment), middle (35th–37th segment) and the tip of the antenna (>70th segment). Segments were counted from excised portion moving distally. For the single odor pulses, chemical signals were measured only in the middle position. In addition, the chemical signals were recorded at three different flow speeds $0.018 \pm 0.0042 \text{ m s}^{-1}$, $0.053 \pm 0.0042 \text{ m s}^{-1}$, and $0.12 \pm 0.0042 \text{ m s}^{-1}$ (mean \pm SEM). Five antennae of each sex were used in the experiment and were subjected to 8-min trials at each of the three flow speeds for the continuous odor signals and ten pulse signals.

The trials were done in a dark room with the antennae illuminated with a Dolan-Jenner Fiber Lite 1990. The trials were video recorded with a Panasonic wv-CL350 camera, onto a Panasonic ag-1980 VCR and displayed on a Sony PVM-1351Q trinitron video monitor.

Chemical signal

The odor source was 4 $\text{mmol}\cdot\text{l}^{-1}$ dopamine, 2 $\text{mmol}\cdot\text{l}^{-1}$ ascorbic acid, and 0.05 $\text{mmol}\cdot\text{l}^{-1}$ fluorescein. The continuous odor signal was stored in a Pyrex reservoir connected to a Pasteur pipette delivery system. The chemical signal was gravity fed at rate 1 ml min^{-1} into the center of the flume through an in-line flow meter (Manostat #2) and a 1.5 mm tip diameter Pasteur pipette. The volume in the reservoir was maintained at a constant level by addition of solution to the reservoir every minute. A pinch-cock was used to terminate flow of chemical signal.

To deliver pulses, a small valve (General Valve 3-111-900) was controlled by a single output stimulator (Grass S48). The valve was opened for 350 ms. Pulses were manually triggered after the previous pulse had been flushed from the boundary layer of the antennae by the flow as measured by IVEC electrode. Ten pulses were recorded for each segment and flow speed. Control trials were performed by removing the antennae and measuring the odor signals with the electrode in the center of the working section.

Data analysis

Different aspects of the temporal chemical signal profile were analyzed using an in-house BASIC program. Signal parameters analyzed included peak height, slope of the signal, length of the signal

(Moore and Atema 1988) and decay time of the signal (time for the signal to decay from peak height to a concentration value of 1% of the peak height). Further details on the other definitions can be found in Moore et al. (1994). Two-way repeated measures ANOVA's with sex and speed as the two factors were used to determine changes in pulse parameters between boundary layer and control. Post-hoc Tukey-HSD multiple comparisons test were used to test for differences when the ANOVA showed significant differences. All significant differences were determined using $P < 0.05$.

A spectral analysis was used to analyze the continuous data using the Fast-Fourier Transform method by a commercial program (Statistica by Statsoft). The spectral analysis of the odor profiles were run on five 91.3-s sequential subsections of the total 7.6-min trials. Subsequently, the five spectral analyses were averaged for each individual animal. Following this, the spectral analysis for each of the five male and five females were separately averaged and normalized to the maximum value within the spectral analysis. This method results in the best estimate of the frequency spectrum, but also includes some loss in frequency resolution (Moore 1994; D. Mountain, personal communication). A Fourier analysis reduces the complex wave form into its component sine waves with different frequencies and amplitudes. This method produces a power-versus-frequency plot. In chemical terms, the onset slope of the chemical signal or frequency of pulses is represented as the frequency band: a steep slope with a short rise time is expressed as a high frequency. The number of pulses or concentration magnitude of those pulses contributes to the 'energy' contained within that frequency band. High concentration pulses or a large number of pulses within a certain frequency band will result in a higher 'energy' portrayed in that band. To provide an idea of the filtering effect that the boundary layer performs on arriving chemical signals, the spectral density results from the controls were subtracted from the antennae trials. The resulting plot shows which aspects of the chemical signal is amplified (positive values) or filtered (negative values) by the physical morphology (Moore 1994).

Results

Pulse signal

Effect of flow on control pulses

For the control odor pulses, both the peak height and onset slope significantly increased as flow velocity increased (Fig. 2; ANOVA, $P < 0.05$). Peak height increased from 1.496 $\mu\text{mol}\cdot\text{l}^{-1}$ (0.018 m s^{-1}) to 2.752 $\mu\text{mol}\cdot\text{l}^{-1}$ (0.05 m s^{-1}) to 3.741 $\mu\text{mol}\cdot\text{l}^{-1}$ (0.12 m s^{-1}). Multiple comparisons showed that each of these means were significantly different from each other (Tukey-HSD, $P < 0.05$). Onset slope increased significantly from 5.95 $\mu\text{mol}\cdot\text{l}^{-1} \text{ s}^{-1}$ (0.018 m s^{-1}) to 10.98 $\mu\text{mol}\cdot\text{l}^{-1} \text{ s}^{-1}$ (0.05 m s^{-1}) to 14.52 $\mu\text{mol}\cdot\text{l}^{-1} \text{ s}^{-1}$ (0.12 m s^{-1}) (ANOVA, $P < 0.05$). There was no significant difference between the slope values at the slow and fast flow speeds compared to the intermediate speed. Conversely, the decay time decreased as the flow speed increased. The decay time at the fastest flow speed (1.1 s) was significantly shorter than the decay times at the intermediate and slowest flow speed (0.9 s and 0.7 s, respectively; ANOVA, Tukey-HSD, $P < 0.05$). Thus, the pulse shape was steeper in slope, higher in concentration, and decayed in a shorter period of time as the flow velocity was increased.

Effect of male and female antennal morphology on pulse signal parameters

All of the peak parameters analyzed in this study for the male and female antennae were significantly greater than the control value (Fig. 2; two-way ANOVA, $P < 0.05$). The peak height was significantly higher for both male and female antennae as compared to control values and female antennae showed a significantly higher peak height than male antennae (Fig. 2A; two-way ANOVA, Tukey-HSD, $P < 0.05$). This difference was apparent and consistent for all three flow speeds. The onset slope was also significantly higher within the boundary layer of the male and female moth antennae as compared to control onset slope. Unlike peak height, the only significant difference between the sexes occurred at the intermediate flow speed (0.05 m s^{-1}). At this flow speed, the onset

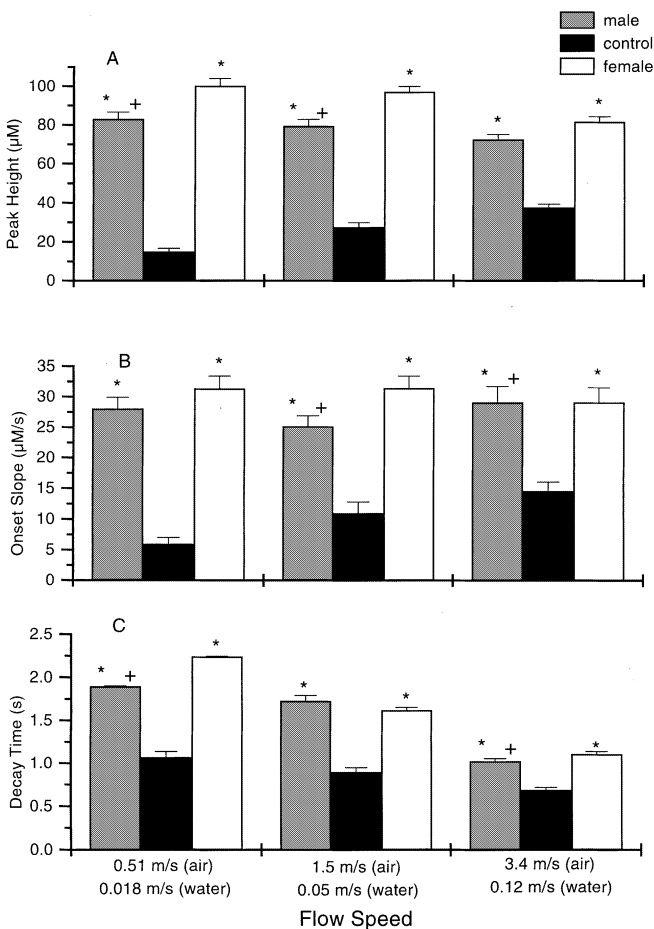


Fig. 2A–C Changes in pulse parameters in the boundary layer surrounding male and female moth antennae at three different flow speeds for single pulses: **A** peak height; **B** onset slope; **C** peak length of the chemical signal for control (black), male antennae (gray), and female antennae (white). Bars represent mean (\pm SEM) for ten pulses each for five antennae. two-way ANOVA with a post-hoc Tukey-HSD test was used to determine significant difference. Asterisks indicate significant differences when compared with controls, while plus indicates a significant difference between sexes. $P < 0.05$ for all tests

slope within the boundary layer around the female antennae was significantly greater than the male onset slope (Fig. 2B; two-way ANOVA, Tukey-HSD, $P < 0.05$). The decay time was significantly longer within the boundary layer of the male and female moth antennae than the decay time during the control experiments. Each of the decay times for all three flow speeds and for both sexes was significantly longer than the control experiments (Fig. 2C). Only the decay time at the slowest and fastest flows showed significant difference between the sexes (two-way ANOVA, Tukey-HSD, $P < 0.05$). The boundary layer surrounding both the male and female antennae significantly increased the peak height, peak slope, and decay time as compared to control values.

Continuous signal

Effect of flow on control odor plumes

For the control odor plumes, the peak height decreased as flow speed increased. Only the peak height at the slowest flow speed was significantly higher than the other two flow speeds (Fig. 3; ANOVA, Tukey-HSD, $P < 0.05$). The onset slope did not significantly change as the flow speed was increased. Conversely, the peak length was significantly longer at the intermediate flow speed (two-way ANOVA, Tukey-HSD, $P < 0.05$), while the peak length at the slowest and fastest flow speeds were not different from each other.

Effect of male and female antennae morphology on odor plume parameters

Base of the antennae At the base of the antennae, the peak height was significantly lower at all three flow speeds for the female antennae when compared to control values (Fig. 3A; two-way ANOVA, Tukey-HSD, $P < 0.05$). The peak height for the male antennae was significantly lower from control values only at the slowest flow speed (Fig. 3A; two-way ANOVA, Tukey-HSD, $P < 0.05$). The peak height for female antennae was significantly higher at the slowest flow speed and was significantly lower at the two faster flow speeds (Fig. 3A; two-way ANOVA, Tukey-HSD, $P < 0.05$). The presence of the boundary layer around the antennae significantly decreased the concentration of odor pulses detected by the electrode, but this effect was different for the male and female morphologies.

The onset slope was significantly decreased at all three flow speeds for both male and female antennae when compared to control values (Fig. 3B; two-way ANOVA, Tukey-HSD, $P < 0.05$). The onset slopes for the female antennae were significantly greater from the onset of the male antennae at the slowest speed, but were significantly less than the onset slopes for the male antennae at the highest flow speed (Fig. 3B; two-way

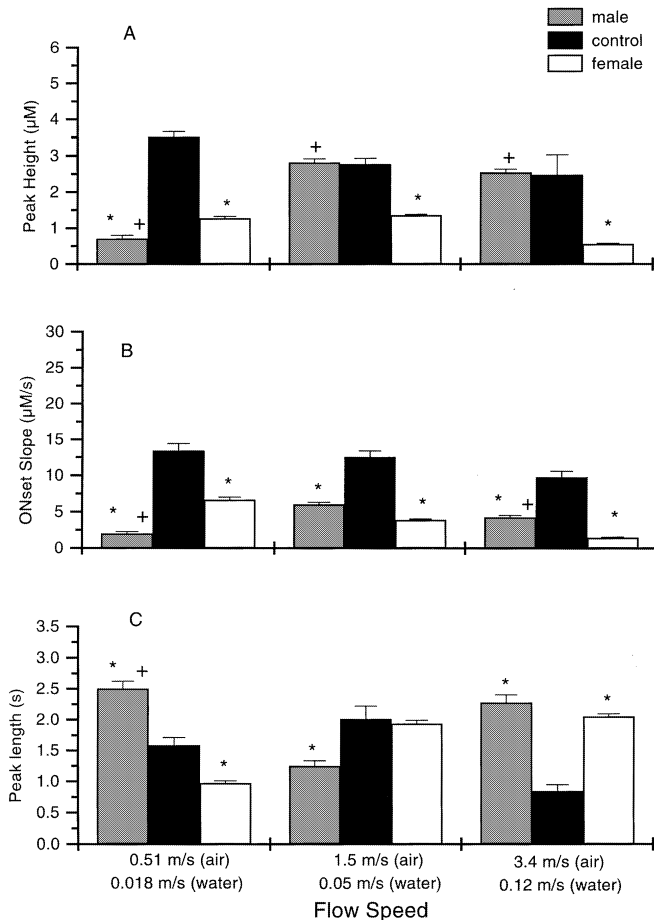


Fig. 3A–C Changes in pulse parameter with the boundary layer at the base of the antenna for a continuous odor source: **A** peak height; **B** onset slope; **C** peak length of the chemical signal for control (black), male antennae (gray), and female antennae (white). Bars represent mean (\pm SEM) for 7.6-min trial for five antennae. Two-way ANOVA with a post-hoc Tukey-HSD test was used to determine significant difference. Asterisks indicate significant differences when compared with controls, while plus indicates a significant difference between sexes. $P < 0.05$ for all tests

ANOVA, Tukey-HSD, $P < 0.05$). As with the peak height, the boundary layer significantly decreased the onset slope of both male and female antennae, but the filtering effect was different for the two morphologies and dependent on the flow speed.

The peak length was significantly different at all three flow speeds for the male and at the slowest and fastest speeds for the female antennae when compared to the control values (Fig. 3C; two-way ANOVA, Tukey-HSD, $P < 0.05$). The female antennae had significantly longer peak lengths than the controls at the fastest flow speed, but the peak lengths were significantly shorter than the controls for the slowest flow speed. The male antennae had significantly longer peak lengths than the controls at the slowest and fastest flow speed, but the peak lengths were significantly shorter than the controls for the intermediate flow speed. The only significant difference between the male and female antennae for peak length occurred at the slowest flow speed (Fig. 3C).

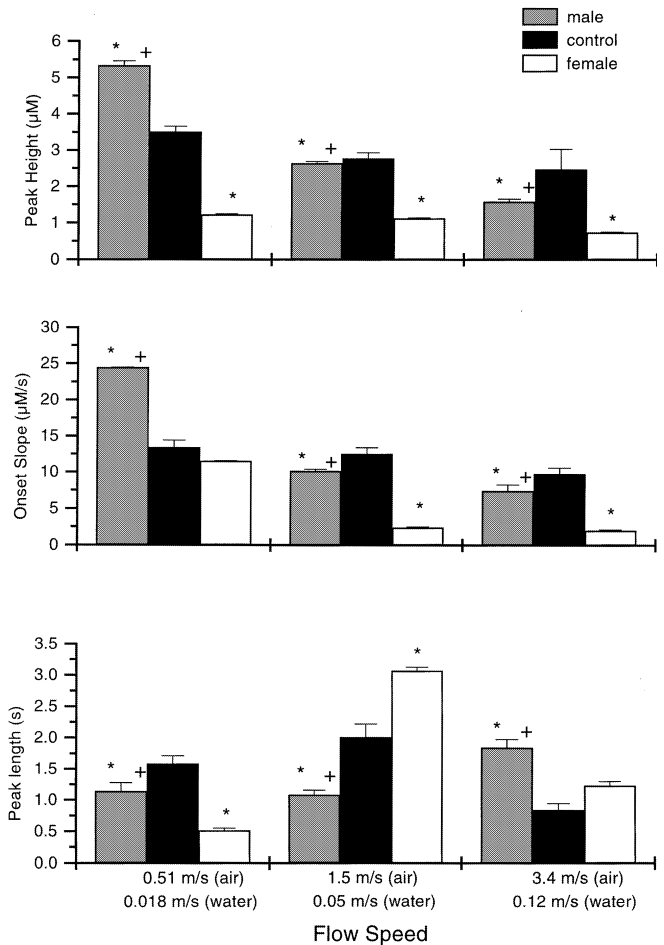


Fig. 4A–C Changes in pulse parameter with the boundary layer at the middle of the antenna for a continuous odor source: **A** peak height; **B** onset slope; **C** peak length of the chemical signal for control (black), male antennae (gray), and female antennae (white). Bars represent mean (\pm SEM) for 7.6-min trial for five antennae. Two-way ANOVA with a post-hoc Tukey-HSD test was used to determine significant difference. Asterisks indicate significant differences when compared with controls, while plus indicates a significant difference between sexes. $P < 0.05$ for all tests

Middle of the antennae The values for the peak height at the middle of the female antennae identically followed the results from the base of the antennae. The peak height for the female antennae was significantly lower at all three flow speeds for the female antennae when compared to control values (Fig. 4A; two-way ANOVA, Tukey-HSD, $P < 0.05$). In addition, the peak height for the male antennae was significantly lower from control values at the intermediate and fastest flow speeds, but was significantly greater at the slowest speed (Fig. 4A; two-way ANOVA, Tukey-HSD, $P < 0.05$). The peak height for female antennae was significantly lower than the peak height for the male antennae at all three flow speeds. The presence of the boundary layer around the antennae significantly changed the concentration of odor pulses detected by the electrode, but this effect was different for the male and female morphologies.

The onset slope was significantly decreased for the intermediate and fastest flow speeds for both male and female antennae when compared to control values (Fig. 4B; two-way ANOVA, Tukey-HSD, $P < 0.05$). At the slowest flow speed, the onset slopes for the female antennae was not different from the control onset slope, but the slope for the male antennae was significantly greater than the control values (Fig. 4B; two-way ANOVA, Tukey-HSD, $P < 0.05$). As with the peak height, the boundary layer significantly decreased the onset slope of both male and female antennae at the two fastest speeds, but the filtering effect was different at the slowest flow velocity.

The peak length was significantly different at all three flow speeds for the male antennae when compared to the control values (Fig. 4C; two-way ANOVA, Tukey-HSD, $P < 0.05$). The peak length was significantly lower for the male antennae at the slowest and intermediate flow speeds, while significantly longer at the fastest flow speed. In addition, the peak length for the male antennae was significantly longer than the peak length for the female antennae at the slowest and fastest speeds, but shorter at the intermediate speeds (Fig. 4C; two-way ANOVA, Tukey-HSD, $P < 0.05$). The female antennae had significantly longer peak lengths than the controls at the intermediate flow speed, but the peak lengths were significantly shorter than the controls for the slowest flow speed.

Tip of the antennae The peak height was significantly lower at all three flow speeds for the female antennae at the tip when compared to control values (Fig. 5A; two-way ANOVA, Tukey-HSD, $P < 0.05$). The peak height for the male antennae was significantly greater than control values only at the slowest flow speed (Fig. 5A; two-way ANOVA, Tukey-HSD, $P < 0.05$). The peak height for male antennae was significantly higher than the female antennae at all three flow speeds (Fig. 5A; two-way ANOVA, Tukey-HSD, $P < 0.05$). The presence of the boundary layer around the antennae significantly decreased the concentration of odor pulses detected by the electrode in the female antennae, but significantly increased the concentration detected in the male antennae.

The onset slope was significantly decreased at all three flow speeds for female antennae when compared to control values (Fig. 5B; two-way ANOVA, Tukey-HSD, $P < 0.05$). The onset slopes for the male antennae were significantly greater from the control onset at the slowest speed, but were significantly less at the fastest flow speed (Fig. 5B; two-way ANOVA, Tukey-HSD, $P < 0.05$). The onset slopes for the male antennae were significantly higher than the onset slopes for the female antennae at all three flow speeds.

The peak length was significantly lower for the slowest and intermediate flow speeds for both the female antennae when compared to the control values and significantly higher at the fastest flow speed (Fig. 5C; two-way ANOVA, Tukey-HSD, $P < 0.05$). The male

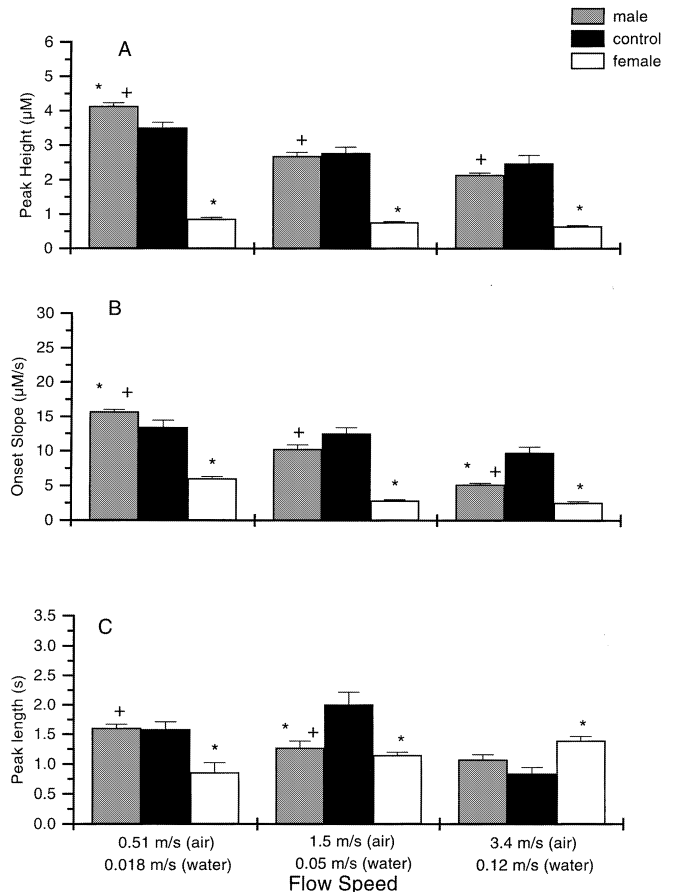


Fig. 5A–C Changes in pulse parameter with the boundary layer at the tip of the antenna for a continuous odor source: **A** peak height; **B** onset slope; **C** peak length of the chemical signal for control (black), male antennae (gray), and female antennae (white). Bars represent mean (\pm SEM) for 7.6-min trial for five antennae. Two-way ANOVA with a post-hoc Tukey-HSD test was used to determine significant difference. Asterisks indicate significant differences when compared with controls, while plus indicates a significant difference between sexes. $P < 0.05$ for all tests

antennae had significantly shorter peak lengths at the intermediate speed, but the peak length was not significantly different at the fastest or slowest speeds. The female antennae had significantly shorter peak lengths than the male antennae for the slowest and intermediate flow speed.

Spectral analysis of odor plumes

The results of the spectral analysis of the odor signal at the fastest flow speed for the male antennae showed a strong amplification of the chemical signal in a narrow frequency band (Fig. 6). The chemical signal near the male antenna at the base and middle position showed the highest amplification of the signal in the range 1.5–2.0 Hz. Near the tip of the antenna there were two prominent points at which the signal was amplified. One was located in the range 0.1–1.0 Hz, while the other was

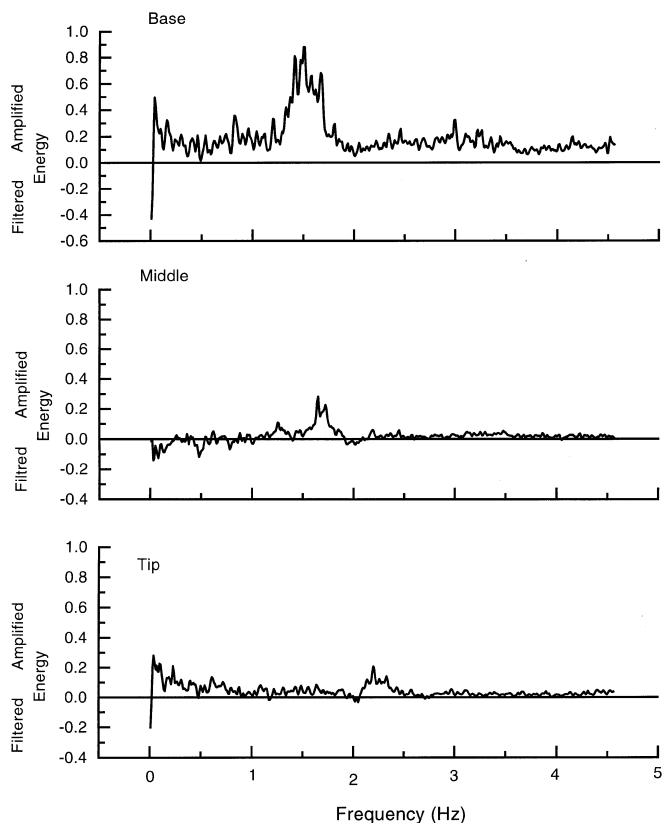


Fig. 6 Spectral density plot of the chemical signal near the male antenna at the flow speed of 0.12 m s^{-1} . The difference plot was created by subtracting the spectral analysis from the control odor plumes from the spectral analysis of the boundary layer influenced odor plumes. *Positive values* indicate amplification of that part of the chemical spectrum, while *negative values* mean that portion of the spectrum is filtered

in the range 2.0–2.5 Hz. All other frequencies were slightly amplified.

The female antenna also amplified specific frequency ranges within the odor plume, but these are different than the ranges amplified by the male antennae. The greatest amplification for the female antennae near the base section occurred in the range 1.0–1.5 Hz. In the middle section, there was a slight amplification in the range 2.0–2.5 Hz, whereas at the tip the signal was filtered (Fig. 7). At the slowest and intermediate flow speeds, there were no intense bands of amplification or filtering shown on the spectral analysis for either the male antennae or the female antennae (not shown).

Discussion

Our results show that the boundary layer structure determined by the morphology of the moth antennae significantly alters the temporal dynamics of the chemical signal arriving at the microenvironment of the receptor cell. The peak height of the chemical signal near the male and female antenna is dramatically increased in concentration at each of the three flow speeds (Fig. 2A).

The onset slope of the chemical signal for the male and female antenna was steeper as compared to the control (Fig. 2B). Due to the boundary layer, the decay time of the chemical signal is significantly longer near the moth antennae than the control signal (Fig. 2C). Thus, all the aspects of the pulsatile chemical signal coming into the microenvironment of the antenna were increased by the boundary layer.

The effect that the boundary layer has in altering the incoming odor signal depends upon the morphology of the antenna. Comparison of the chemical signal dynamics for the different morphologies of the male and female antenna using the pulsatile data showed that female antenna have a higher peak height within the boundary layer than the male antenna (Fig. 2A). The onset slope for the chemical signal in the boundary layer around the female antenna was significantly greater than the onset slope of the chemical signal near the male antenna at the intermediate flow speed (Fig. 2B). The decay time for the chemical signal near the female antenna was significantly longer than the male morphology at the slow flow speed (Fig. 2C). The chemical signal near the female antenna is faster, stronger and longer than the signal near the male antenna. Thus, the

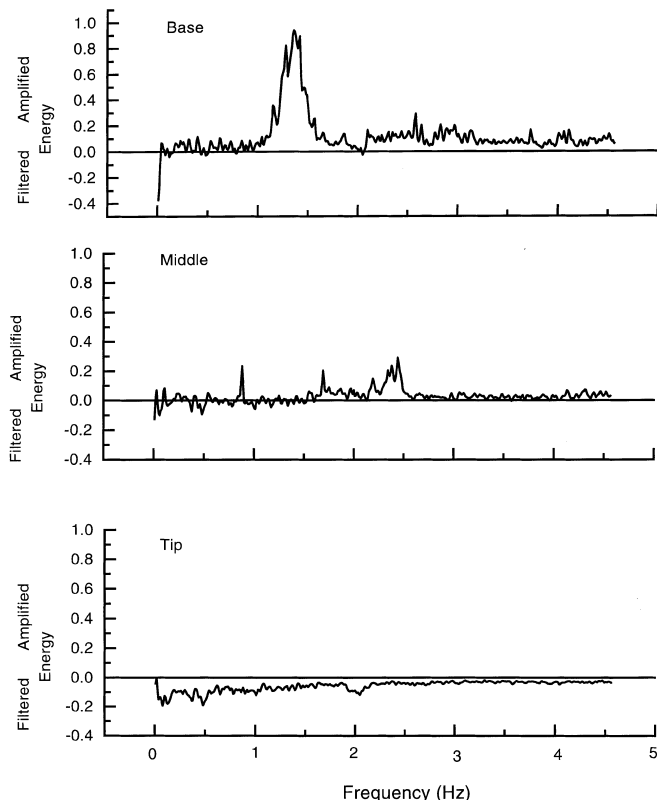


Fig. 7 Spectral density plot of the chemical signal near the female antenna at the flow speed of 0.12 m s^{-1} . The difference plot was created by subtracting the spectral analysis from the control odor plumes from the spectral analysis of the boundary layer influenced odor plumes. *Positive values* indicates amplification of that part of the chemical spectrum, while *negative values* mean that portion of the spectrum is filtered

boundary layer surrounding the male antenna alters the dynamics of the odor signal differently than the boundary layer around the female antenna.

It is clear from these results that the boundary layer surrounding a moth antennae will act as a biomechanical filter by altering the temporal and concentration dynamics of odor signals as they are transported from the environment to the receptor cells. The temporal dynamics of the chemical signal are a result of the flow patterns (i.e., Re number) and to a smaller degree the interaction between molecular diffusion and fluid flow (i.e., Pe number). The boundary layer changes both the flow patterns and the Pe number. Consequently, the boundary layer changes the temporal dynamics of the chemical signal. By altering the dynamics of the chemical signal that are originally determined by the environment, the boundary layer acts as a filter. Depending on the nature of this filter, it may extract or enhance different temporal aspects of the odor signal. Organisms with different morphologies will have different boundary layers and thus have biomechanical filters with different properties.

The natural signal for these organisms is not single discrete pulses but is a turbulent odor plume. A turbulent odor plume contains a very patchy spatial and temporal distribution of chemical signals (Murlis et al. 1991; Moore et al. 1994). Many studies have shown that there is important spatial and temporal information within this patchy distribution (Moore and Atema 1991; Murlis et al. 1991). The exact nature of the patchy distribution, and consequently the information contained therein, is a direct result of the turbulence that causes chemical dispersion. Odor plumes generated under different turbulence regimes will have different chemical fluctuations in that plume (Murlis et al. 1991; Moore et al. 1994). For moths specifically, this means that the turbulence generating an odor plume originating from a calling female will be quite different from the turbulence creating a plume from a host plant. Since the turbulence is different for these two situations, the temporal fluctuations in the chemical signal will also be different.

Within turbulent odor plumes, our results show that the boundary layer acts as a temporal filter enhancing and/or filtering specific parts of the fluctuating odor signal. For both males and females, the boundary layer results in a strong amplification of the chemical signal in a narrow frequency band (Figs. 6, 7). Chemical signals that are within these narrow bands are amplified, whereas those fluctuations outside of this band are filtered by the morphology of the antenna. The male and female antennae differ in how the boundary layer filters or amplifies signal fluctuations.

The continuous signal results show that both the onset slope and length of the chemical signal changes drastically along the length of the male antennae (Figs. 3B, 4B, 5B). In addition, the peak height, peak length, and onset slope changes along the length of the female antennae (Figs. 3, 4, 5). The differences between the signal within the boundary layer and the environ-

mental signal suggest the boundary layer significantly alters the spatial and temporal structure of the chemical signal that is perceived by the organism within a turbulent plume. The changes in signal structure between the male and female antennae demonstrates that the different morphology between the sexes results in a different filtering effect by the boundary layer even within the same turbulent plume structure. In addition, receptor cells located at different points along the same antennae of a single organism will be exposed to different temporal signal fluctuations and possibly different types of chemical information.

Wehner (1987) has proposed the idea of a 'matched filter' for sensory systems. This hypothesis states that the physical and physiological properties of a sensory system are 'matched' or tuned to that part of the sensory environment that carries the most relevant information. Perceiving the environment through a matched filter helps limit the amount of extraneous and irrelevant information arriving to the nervous system and "frees up the CNS from intricate computations to extract information needed for fulfilling a particular task" (Wehner 1987). If we apply this matched-filter hypothesis to the filtering effect of the boundary layer, we would expect that the boundary layer around the male antenna to enhance those chemical fluctuations that are most prevalent during upwind flight to a pheromone point source, i.e., a calling female. Similarly, it follows from the same hypothesis that the boundary layer around the female antenna should enhance those fluctuations that are most important to locating relevant resources, i.e., a host plant leaf or flower. The differences in the turbulent structure of these two plume situations coupled with the matched-filter hypothesis may help explain from an evolutionary perspective, why the boundary layer surrounding the male antennae functions as a different temporal filter than the boundary layer surrounding the female antennae. We are limited in following this line of reasoning any further due to the lack of the relevant statistical analysis (i.e., spectral analysis) of terrestrial plume measurements (Murlis and Jones 1981; Murlis et al. 1991).

Both female and male moths use turbulent odor plumes to find odor sources, such as calling females or host plants (see reviews by Cardé 1984; Kennedy 1986). These plumes differ, however, in the type of turbulence generated at the odor source. The male moth is responding to odor plumes from single point sources, i.e., a calling female, typically located on a single solid structure (i.e., branch or trunk; M.A. Willis personal communication). Under typical dispersion conditions with flow speeds of 2 m s^{-1} and a characteristic length scale of 0.2 m (Willis et al. 1994), this plume has a Re number $\approx 10^4$ and Pe number ≈ 10 . In contrast, the female moth searching for a host plant is responding to a turbulent odor plume from a much larger odor source. In the Sonoran desert, *Manduca* spp. females are often seen orienting to *Datura wrightii*. If we assume that a patch of *Datura wrightii* has a cross-section of 1.0 m

(order of magnitude estimate) in a flow of 2 m s^{-1} , this would result in a Re number $\approx 10^5$ and a Pe number ≈ 80 . The Re and Pe numbers indicate a difference in the turbulent structure, and consequently a difference in the temporal signal fluctuations under which these animals are orienting.

Some exciting recent work has demonstrated that temporal information of odor signals is particularly important for controlling the upwind flight behavior of certain moths (Vickers and Baker 1992, 1994; Mafra-Neto and Cardé 1994, 1995). The pulsatile nature of the chemical signal, and in particular, the timing associated with the arrival of odor filaments is important in mediating either upwind flight or casting behavior of the moths. The key feature within the odor signal is the frequency information associated with the turbulent nature of odor plumes. All of these studies have modulated the pulsatile nature of the chemical signal at the source and have measured either neurophysiologically (Vickers and Baker 1994) or behaviorally the resulting signal down wind (Mafra-Neto and Cardé 1994). It therefore becomes difficult to place our results within the context of these studies because our study is designed to measure only one filter, the boundary layer. Their indirect measure of the temporal information include the summation of several physical and physiological filters, such as turbulent dispersion, boundary layer filtering, and the adaptation of peripheral chemoreceptor cells.

The turbulent structure determines the type of fluctuations in concentration that occur within an odor plume and sets constraints upon the temporal nature of signals that are available for the animals to use for information. The differences in the ultrastructure of the antennae between the sexes may reflect, in part, a selection pressure for a biomechanical filter that enhances that part of the odor signal that contains the most relevant information for orientation purposes. Therefore, just as receptor cells are 'spectrally-tuned' to relevant chemicals within the environment (Derby and Atema 1988), the boundary layer structure that is determined by antennal morphology may be 'temporally tuned' to those chemical fluctuations that are most prevalent or behaviorally relevant within the environmental signals.

In addition, these moths have the ability to both change their flying speed and to manipulate the orientation of the antennae with respect to flow during flight (M.A. Willis, personal communication). Both of these behavioral adjustments during orientation will alter the thickness and structure of the boundary layer. This, in turn, will change the filtering effect that the boundary layer has on incoming chemical signals. Thus, during any single orientation flight, the exact filtering performed by the boundary layer will change moment by moment. If the moths are actively changing the antennal orientation with respect to flow during flight, they may have the ability to control the amount and type of temporal filtering performed by the boundary layer. This could be done through a sensory feedback mechanism

based on the types of information being processed at the periphery or centrally (Kaissling 1985; Christensen and Hildebrand 1988).

This idea of controlling chemosensory input through the manipulation of biomechanical filters has been proposed for other animals (Atema 1988). Most notably, crustaceans can control the filtering done by the boundary layer by controlling the fluid motion and boundary layer thickness around lateral antennules. Crustaceans can control the boundary layer thickness by flicking their antennules (Snow 1973). This serves to increase local velocities, decrease boundary thickness and increase chemical signal transport (Moore et al. 1991). Some fish also control fluid flow over receptor appendages which allow them to control chemosensory input (Døving et al. 1977). Sniffing by aquatic and terrestrial vertebrates increases the fluid velocities in the nasal cavity, changing the boundary layer (Kux et al. 1985).

Although our study was done on only a single orientation (normal to flow), only at set speeds, and on fully developed boundary layers, it serves as a stepping stone for further research on biomechanical filters in chemosensory biology. The data presented here provides a look at the spatial and temporal profile of the chemical signal near the microenvironment of the receptor cell and how fluid flow around the moth antennae can alter the temporal dynamics that are available to receptor cells. This study can provide some insight into the true structure of chemical signals as they are being transported from the environment at the odor source to the small scale environment around receptor cells.

Finally, chemical signals are composed of four different components that carry potential information for an organism: (1) quality (or chemical composition), (2) intensity (or molecular contacts per unit time), (3) spatial distribution, and (4) temporal distribution. Many physiological investigations on the filtering properties of peripheral chemoreceptor cells and neurons in the CNS (Kaissling et al. 1987; Christensen and Hildebrand 1988) along with numerous studies on orientation behavior (Vickers and Baker 1992, 1994; Mafra-Neto and Cardé 1994, 1995) have demonstrated the importance of signal intensity, spatial distribution, and temporal distribution for insect chemosensory behavior. While these studies have been critical for advancing our knowledge of insect behavior, they have made the assumption that the same signals that are being introduced into the environment are also arriving at the receptor cells. None of these studies have actually measured the signal structure as it arrives to the receptor cells. Our current study demonstrates that it is transport through the boundary layer surrounding chemosensory structures that ultimately determines these signal characteristics that are either evoking the neural responses measured in these studies or guiding the observed orientation behavior. Thus, before any definite conclusions can be drawn on how these signal properties guide insect decision making, it is imperative to understand how the boundary layer can

alter the intensity, spatial distribution or temporal distribution that is arriving at the receptor cells.

In summary, the interaction of fluid flow with the antenna's morphology functions as a physical filter for chemical signals. The boundary layer alters the chemical signal into a new spatial and temporal profile as it arrives at the receptor cell. This physical filter may be "temporally tuned" to the relevant chemical signal fluctuations within the environments where the *M. sexta* resides. In addition, the sexual dimorphism of antennal morphologies may be, in part, due to the different environmental constraints that are present in the different turbulent odor plumes.

Acknowledgements The authors would like to thank T.A. Clason, S. Francoeur, and G. Buehner for reading early revisions of the manuscript and Dr. S. Smith who provided us with his expertise in raising the *Manduca sexta*. This study was funded by a NSF grant to P.M. (NSF IBN-9514492).

References

- Adam G, Delbrück M (1968) Reduction of dimensionality in biological diffusion processes. In: Rich A, Davidson N (eds) Structural chemistry and molecular biology. Freeman, San Francisco, pp 198–215
- Adams RN (1969) Electrochemistry at solid electrodes. Dekker, New York
- Adamson AW (1973) A textbook of physical chemistry. Academic Press, New York
- Atema J (1985) Chemoreception in the sea: adaptations of chemoreceptors and behaviour to aquatic stimulus conditions. In: Laverack MS (ed) Society of experimental biology symposium 39. Company of Biologists, Cambridge, pp 387–423
- Atema J (1988) Distribution of chemical stimuli. In: Atema J, Fay RR, Popper AN, Tavolga WM (eds) Sensory biology of aquatic animals. Springer, Berlin Heidelberg New York, pp 29–56
- Bell RA, Joachim FA (1976) Techniques for rearing laboratory colonies of tobacco hornworms and pink bollworms. *Ann Entomol Soc Am* 69: 365–373
- Berg HC (1993) Random walks in biology. Princeton University Press, Princeton, New Jersey
- Cardé RT (1984) Chemo-orientation in flying insects. In: Cardé RT, Bell WJ (eds) Chemical ecology of insects. Sinauer, Sunderland, Mass., pp 111–126
- Cheer AYL, Koehl MAR (1987) Paddles and rakes: fluid flow through bristled appendages of small organisms. *J Theor Biol* 129: 17–39
- Christensen TA, Hildebrand JG (1988) Frequency coding by central olfactory neurons in the sphinx moth *Manduca sexta*. *Chem Senses* 13: 123–130
- Derby CD, Atema J (1988) Chemoreceptor cells in aquatic invertebrates: peripheral mechanisms of chemical signal processing in decapod crustaceans. In: Atema J, Popper AN, Fay RR, Tavolga WN (eds) Sensory biology of aquatic animals. Springer, Berlin Heidelberg New York, pp 365–385
- DeSimone JA (1981) Physiochemical principles in taste and olfaction. In: Cagen RH, Kare MR (eds) Biochemistry of taste and olfaction. Academic Press, New York, pp 213–229
- Døving KB, Dubois-Dauphin M, Holley A, Jourdan F (1977) Functional anatomy of the olfactory organ of fish and the ciliary mechanism of water transport. *Acta Zool* 58: 245–255
- Futrelle RP (1984) How molecules get to their detectors: the physics of diffusion of insect pheromones. *TINS* 94: 116–119
- Gerhardt GA, Oke AF, Nagy G, Moghaddam B, Adams RN (1984) Nafion-coated electrodes with high selectivity for CNS electrochemistry. *Brain Res* 290: 390–395
- Gerhardt GA, Rose GM, Hoffer BJ (1987) In vivo electrochemical demonstration of potassium-evoked monoamine release from rat cerebellum. *Brain Res* 413: 327–335
- Kaissling KE (1985) Temporal characteristics of pheromone receptor cell responses in relation to orientation behavior of moths. In: Payne TL, Birch MC, Kennedy CEJ (eds) Mechanisms in insect olfaction. Clarendon Press, Oxford, pp 193–199
- Kaissling K-E, Zack-Strassfeld C, Rumbo E (1987) Adaptation processes in insect olfactory receptors: mechanisms and behavioral significance. In: Roper S, Atema J (eds) Olfaction and Caste IX. *N Y Acad Sci* 510: 104–112
- Kennedy JS (1986) Some current issues in orientation to odour sources. In: Payne TL, Birch MC, Kennedy CEJ (eds) Mechanisms in insect olfaction. Clarendon Press, Oxford, pp 11–25
- Keogh DP, Smith SL (1991) Regulation of cytochrome p-450 dependent steroid hydroxylase activity in *Manduca sexta*: effects of ecdysone agonist RH5849 on Ecdysone 20-Monooxygenase activity. *Biochem Biophys Res Comm* 176: 522–527
- Koehl MAR (1993) Hairy little legs: feeding, smelling, and swimming at low Reynolds numbers. *Contemp Math* 141: 33–64
- Koehl MAR (1995) Fluid flow through hair-bearing appendages: feeding, smelling and swimming at low and intermediate Reynolds numbers. In: Pedley T, Ellington C (eds) Biological fluid dynamics. *Symp Soc Exp Biol* 27: pp 157–182
- Koehl MAR (1996) Small-scale fluid dynamics of olfactory antenna. *Mar Freshwater Behav Physiol* 27: 127–141
- Kux J, Zeiske E, Osawa Y (1988) Laser Doppler velocimetry measurement in the model flow of a fish olfactory organ. *Chem Senses* 13: 257–265
- Mafra-Neto A, Cardé RT (1994) Fine-scale structure of pheromone plumes modulates upwind orientation of flying moths. *Nature* 369: 142–144
- Mafra-Neto A, Cardé RT (1995) Influence of plume structure and pheromone concentration on the upwind flight of *Cadra cautella* males. *Physiol Entomol* 20: 117–133
- Moore PA (1994) A model of the role of adaptation and disadaptation in olfactory receptor neurons: implications for the coding of temporal and intensity patterns of odor signals. *Chem Senses* 19: 71–86
- Moore PA, Atema J (1988) A model a temporal filter in chemoreception to extract directional information from a turbulent odor plume. *Biol Bull* 174: 355–363
- Moore PA, Atema J (1991) Spatial information in the three-dimensional fine structure of an aquatic odor plume. *Biol Bull* 181: 408–418
- Moore PA, Gerhardt GA, Atema J (1989) High resolution spatio-temporal analysis of aquatic chemical signals using microelectrochemical electrodes. *Chem Senses* 14: 829–840
- Moore PA, Atema J, Gerhardt GA (1991) Fluid dynamics and microscale chemical movement in the chemosensory appendages of the lobster, *Homarus americanus*. *Chem Senses* 16: 663–674
- Moore PA, Zimmer-Faust RK, BeMent SL, Weissburg MJ, Parrish JM, Gerhardt GA (1992) Measurement of microscale patchiness in a turbulent aquatic odor plume using a semiconductor-based microprobe. *Biol Bull* 183: 138–142
- Moore PA, Weissburg MJ, Parrish JM, Zimmer-Faust RK, Gerhardt GA (1994) Spatial distribution of odors in simulated benthic boundary layer flows. *J Chem Ecol* 20: 255–279
- Murlis J, Jones CD (1981) Fine-scale structure of odour plumes in relation to insect orientation to distant pheromone and other attractant sources. *Physiol Entomol* 6: 71–81
- Murlis J, Willis MA, Cardé RT (1991) Odour signals: patterns in space and time. In: Døving K (ed) Proceedings of the tenth international symposium on olfaction and taste. Graphic Communication System, Oslo, pp 6–17
- Schlichting H (1987) Boundary Layer Theory, 7th edn. McGraw-Hill, New York
- Snow PJ (1973) The antennular activities of the hermit crab, *Pagurus alaskiensis* (Benedict). *J Exp Biol* 58: 745–766

- Vickers NJ, Baker TC (1992) Male *Heliothis virescens* maintain upwind flight in response to experimentally pulsed filaments of their sex pheromone (Lepidoptera: Noctuidae). *J Insect Behav* 5: 669–687
- Vickers NJ, Baker TC (1994) Reiterative responses to single strands of odor promote sustained upwind flight and odor source location by moths. *PNAS* 91: 5756–5760
- Vogel S (1983) How much air passes through a silkworm's antenna? *J Insect Physiol* 29: 597–602
- Vogel S (1994) *Life in moving fluids: the physical biology of flow*. Princeton University Press, Princeton, New Jersey
- Wehner R (1987) 'Matched filters' – neural models of the external world. *J Comp Physiol A* 161: 511–531
- Willis MA, David CT, Murlis J, Cardé RT (1994) Effects of pheromone plume structure and visual stimuli on the pheromone-modulated upwind flight of the male gypsy moths (*Lymantria dispar*) in a forest (Lepidoptera: Lymantriidae). *J Insect Behav* 7: 385–409
- Zimmer-Faust RK, Stanfill JM, Collard SB III (1988) A fast, multichannel fluorometer for investigating aquatic chemoreception and odor trails. *Limnol Oceanogr* 33: 1586–1595